Spectrochimica Acta Part A: Molecular and Biomolecular Spectroscopy 207 (2019) 132–142

Contents lists available at ScienceDirect

Spectrochimica Acta Part A: Molecular and Biomolecular Spectroscopy

journal homepage: www.elsevier.com/locate/saa

Conformational study of the electronic interactions and nitric oxide release potential of new *S*-nitrosothiols esters derivatives of ibuprofen, naproxen and phenyl acids substituted (SNO-ESTERS): Synthesis, infrared spectroscopy analysis and theoretical calculations

Marcelo Mota Reginato [a], Derisvaldo Rosa Paiva [a], Fabrício Ronil Sensato [a], Hugo Pequeno Monteiro [b], Adriana Karla Cardoso Amorim Reis [a,*]

[a] Department of Chemistry, Institute of Environmental, Chemical and Pharmaceutical Sciences, Universidade Federal de São Paulo – Campus Diadema, Brazil
[b] Department of Biochemistry, Center for Cellular and Molecular Therapy, Universidade Federal de São Paulo – Campus São Paulo, Brazil

ARTICLE INFO

Article history:
Received 26 May 2018
Received in revised form 8 September 2018
Accepted 10 September 2018
Available online 11 September 2018

Keywords:
S-Nitrosothiols
Nitric oxide
Synthesis
Infrared spectroscopy
Theoretical calculations
Natural Bond Orbital

ABSTRACT

The conformational study on the new *S*-nitrosothiols esters (SNO-ESTERS): *para*–substituted (X = H, OMe, Cl and NO_2) *S*-nitrosothiol derivatives 2-methyl-2-(sulfanyl)propyl phenylacetates (**R1**), 2-(4-isobutylphenyl) propanoate (ibuprofen, **R2**), and 2-(4-isobutylphenyl)propanoate of 2-methyl-2-(nitrososulfanyl)propyl (naproxen, **R3**) was performed using infrared spectroscopy (IR) in solvents with increasing polarity (CCl_4, CH_3Cl, and CH_3CN), and theoretical calculations, to determine the preferential conformer and the potential of these compounds to release nitric oxide (NO). *S*-Nitrosothiols were synthesized by esterification reactions, using chlorides of the corresponding carboxylic acids, with good yields (~60%). IR results showed that these compounds presented only one conformation, and the experimental data were supported by the theoretical results obtained by density functional theory (DFT) calculations using the 6311+G (2df, 2p) basis set. The calculations revealed that all *S*-nitrosothiols presented one preferential *anticlinal* (*ac*) geometric conformation, which agrees with the data obtained experimentally in CCl_4. These conformers are stabilized by intramolecular hydrogen bonds. Examination of the geometry with regard to the R—SNO group revealed that these compounds are preferentially in the *trans* (*anti*) conformation. The calculation of the orbital interactions using the Natural Bond Orbital (NBO) method showed that the $n_{O(NO)} \rightarrow \sigma^*_{(S-N)}$ hyper-conjugative interaction increases the S—N bond length. The strong $n_S \rightarrow \pi^*_{(NO)}$ interaction and electronic delocalization induces a partial π character to the S—N bond. The weak σ_{S-N} bond indicates strong delocalization of the electron pair in O (NO) by the $n_{O(NO)} \rightarrow \sigma^*_{(S-N)}$ interaction, thereby increasing the capacity of NO release from SNO-ESTERS.

1. Introduction

Non-steroidal anti-inflammatory drugs (NSAIDs) are effective in the treatment of pain, fever, and inflammation. NSAID–based therapy effectively reduces the symptoms of many painful arthritic syndromes. However, side effects involving damage to the patient's gastrointestinal tract during NSAID therapy are frequently reported. The most common clinical manifestation of NSAID-related damage is a combination of gastroduodenal erosions and ulcerations, often called NSAID-induced gastropathy, affecting at least 15% of chronic NSAID users [1–3].

During the 1990s, several structurally diverse compounds derived from NSAID and displaying gastro sparing properties in rodents were synthesized. The important strategy used to improve the NSAID safety profile was coupling a nitric oxide (NO) donor group to the NSAID [4–6]. NO released from NO-derivatives of NSAID, promotes vasodilatation of veins and arteries, inhibits platelet aggregation, and reduces the formation of blood clots [6,7]. In addition, it has been shown that NO exerts beneficial effects to the gastrointestinal (GI) tract, maintaining the integrity of the gastric mucosal barrier [4,5,8].

Different chemical strategies have been used to provide NSAIDs with the capacity to release NO. Nitrooxybutyl-ester derivatives of NSAID display anti-inflammatory activity comparable to the respective parental NSAID against acute inflammation in rodent models, but with reduced GI toxicity [9].

NCX-4016, also called NO-aspirin, is the prototype of an NO-releasing NSAID and consists of the parental aspirin molecule linked via an ester to an NO moiety. Both aspirin and NO moieties of NCX-4016 contribute to its effectiveness, with the effect of the latter

* Corresponding author at: Rua Prof. Artur Riedel, 275, CEP: 09972-270 Diadema, São Paulo, Brazil.
E-mail address: adriana.amorim@unifesp.br (A.K.C.A. Reis).

https://doi.org/10.1016/j.saa.2018.09.020
1386-1425/

occurring via both cyclic GMP-dependent and -independent mechanisms. Human studies have shown that, while NO-aspirin maintains its anti-thrombotic activity, it spares the GI tract. The use of NCX-4016 results in a 90% reduction of the gastric damage caused by equimolar doses of aspirin [10,11].

S-Nitrosation, the NO-mediated modification of sulfhydryl residues of peptides and proteins has been associated with the anti-inflammatory actions of NO-aspirin and NO-naproxen [12,13]. Furthermore, recent studies have shown that *S*-nitrosation of the signaling proteins Src, EGFR, and Ras generating their *S*-nitrosothiols derivatives, regulates pathways associated with cell survival and proliferation (reviewed in [14]).

In addition to NO-NSAIDS, *S*-nitrosothiols are a class of NO donors that under appropriate conditions decompose to liberate NO. They decompose by thermal and photochemical reactions to give the corresponding disulfide and NO. It was proposed that the photolytic decomposition of *S*-nitrosothiols is a two-step process: the first step being the homolytic dissociation of the S—N bond to form •NO and RS• radicals, followed by dimerization of RS• forming the disulfide RSSR [15]. On the other hand, in aqueous buffers at physiological pH, *S*-nitrosothiols decompose in the presence of trace transition metal ions generating NO and RSSR. In this process RS• radicals are not formed [16].

By the reasons explained above, addition of an *S*-nitrosothiol moiety to NSAIDs may prove to be advantageous to these molecules. However, syntheses of these derivatives have been scarcely reported [17].

Theoretical approaches combined with experimental approaches, provide a new and consistent picture of the conformational behavior of *S*-nitrosothiols. The combination of methodologies also provides information on how the conformational behavior influences *S*-nitrosothiols spectroscopic and chemical properties. For instance, to assign the structure of *S*-nitroso-methanethiol, reported calculations showed for B3LYP/6-311+G* calculation minima for the *syn* and *anti* conformations (the former possessing an eclipsed C—H bond). MP2/6-311+G* geometry optimizations and QCISD (T)/6-311+G* single-point calculations further confirm the *syn* preference. Also of note is the preferred eclipsing of an R-CH and *anti-clinal* orientation of the alkyl chain with respect to the SNO moiety in *syn* exclusively in the *anti*-orientation [18].

The reliability and accuracy of the conventional electron correlation methods MP2 and QCISD, and the density functional theory methods B3LYP and B3P86, to obtain optimized structures and homolytic bond dissociation energies S—N of a range of *S*-nitrosothiols, has been investigated. A variety of model RSNOs (HSNO, CH_3SNO, C_2H_3SNO, C_2H_5SNO, C_6H_5SNO, and CysSNO (*S*-nitroso-cysteine) have been used. For all methods considered, optimized S—N bond lengths were found to be highly dependent on the basis set being employed. In general, to obtain convergence in the r(S—N) values of RSNO for a given method, the 6-311$^+$(2df,p) or larger basis set was required [19].

The combination of IR spectroscopy and theoretical calculations has been extensively employed in conformational studies of carbonyl compounds. Analysis of the carbonyl stretching frequencies (ν_{CO}) in solution determines the different conformations assumed by the compounds. The unusual solvent effect and ν_{CO} shifts for the conformers as compared to other α-hetero-substituted carbonyl compounds are interpreted in terms of a decrease in polarity [20–22].

The presence of carbonyls in the structure of an *S*-nitrosothiol might interfere with its conformational behavior. However, potential interference of these groups on the conformational behavior of *S*-nitrosothiols has not been evaluated.

In this work we synthesized the *S*-nitrosothiols 2-methyl-2-(nitrososulfanyl) propyl-phenylacetate-*para*-substituted **R1**, 2-methyl-2-(nitrosothio)-propyl-2-(4-isobutylphenyl)-propanoate **R2** (derivative of ibuprofen), and 2-methyl-2-(nitrosothio) propyl-2-(6-methoxynaphthalen-2-yl)propanoate (derivative of naproxen) **R3**. A conformational study of the compounds was carried out using IR spectroscopy and theoretical calculations. This combination of experimental and theoretical approaches, allowed us to determine the most stable conformation they can assume in relation to the carbonyl group and their potential as NO releasing compounds.

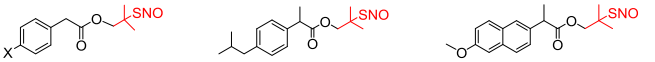

R1 (X=OMe, H, Cl) **R2 (Ibuprofen derivative)** **R3 (Naproxen derivative)**

The compounds showed in solvents of different dielectric constants (CCl_4, CH_3Cl and CH_3CN) only one band in the carbonyl region in most cases. We carried out the conformational search for the studied compounds and stable conformations geometries were theoretically optimized using the B3LYP/DFT/G-6311+ (2df, 2p) basis set. Results obtained in the IR analysis were compared with the theoretical data showing good agreement with experimental results in CCl_4 for isolated molecules. Calculations of orbital interactions using the method of *Natural Bond Orbital* (NBO) showed no electronic interactions capable of stabilizing the SNO-ESTERS conformations, potentially enhancing their ability in releasing NO.

2. Materials and Methods

2.1. S-Nitrosothiols Synthesis

S-Nitrosothiols (**R1**–**R3**) were prepared using the method presented in Scheme 1. The reaction of intermediate **2**, obtained from the reaction of compound **1** with potassium thioacetate (KSAc) in acetone, for 2 h with reflux and with excess of $LiAlH_4$, led to the total reduction of the thioacetate group (-SAc) to thiol (-SH), along with the reduction of the ester group to alcohol (**3**). The *S*-nitrosylation reaction using *t*-butylnitrite (*t*-BuONO) led to the intermediate **4**, which underwent coupling with the carboxylic acids chlorides, precursors of the compounds of interest. All *S*-nitrosothiols, **R1**–**R3**, were obtained in moderate to good yields (45–60%) [23].

Each compound was purified by column chromatography on silica gel using hexane/ethyl acetate as eluent. The structures of all compounds were determined by ^{1}H NMR, ^{13}C NMR, MS (ESI) and IR (Supporting information).

Compounds **R1**–**R3** are stable green oils at room temperature for more than one month. Compounds should be kept in closed vials and protected from light.

2.2. Infrared Spectroscopy

Infrared measurements on the solutions were performed using the FT-IR Michelson Bomem™ MB100 spectrometer, with 1.0 cm^{-1} resolution, between 4000 and 600 cm^{-1}. The solutions were properly prepared with 0.02 $mol \cdot L^{-1}$ concentration in CCl_4, CH_3Cl, and CH_3CN. For the measurements of carbonyl stretch band, we used NaCl cell with a 0.5 mm optical path. The determinations in the first harmonic region were obtained in a quartz cell with 1.0 cm optical path in CCl_4. We used the GRAMS/4.04 program for analyzing the bands [24]. The population of conformers was estimated from the maximum of each component of the resolved carbonyl doublet or triplet. The population of conformers was expressed as a percentage of the absorbance, assuming equimolar absorptivity coefficients for the referred conformers.

2.3. Computational Methods

Calculations were obtained using the Gaussian 09 program [25], in Linux environment, 64-bits Ubuntu, with three servers, two of which contained 16 processors in two Intel® Xeon eight-core E5-26770 sockets of 2.6 GHz, 128 GB RAM, and 9-TB disk, while the other contained two Intel® Xeon® six-core 5560 sockets, 12 processors with 96 GB of RAM, and 3-TB disk.

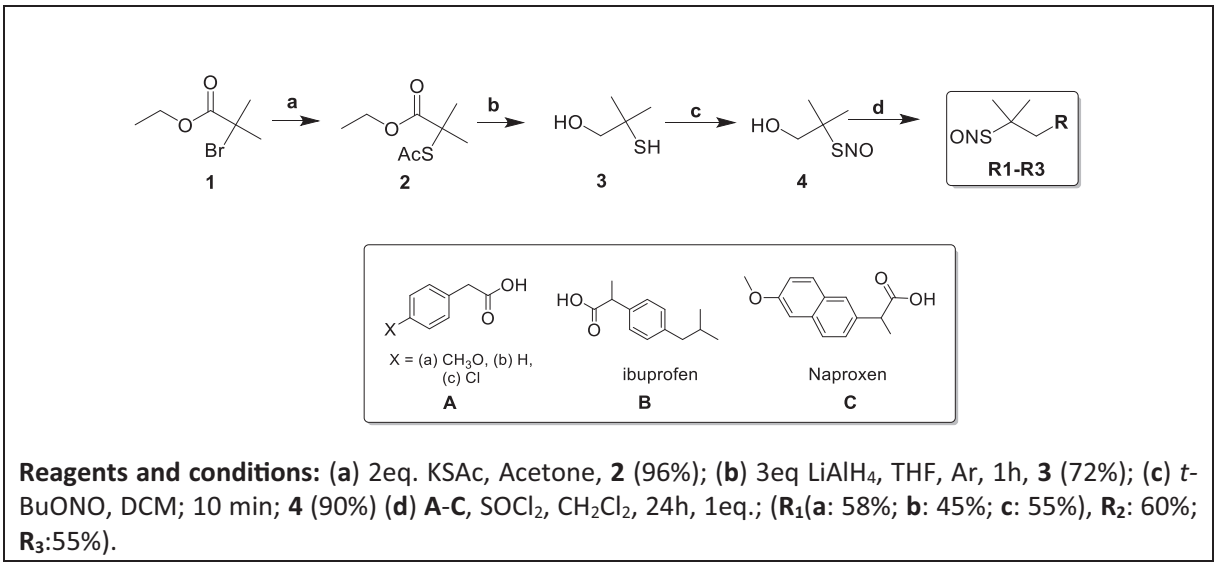

Reagents and conditions: (**a**) 2eq. KSAc, Acetone, **2** (96%); (**b**) 3eq $LiAlH_4$, THF, Ar, 1h, **3** (72%); (**c**) *t*-BuONO, DCM; 10 min; **4** (90%) (**d**) **A**-**C**, $SOCl_2$, CH_2Cl_2, 24h, 1eq.; (**R_1**(**a**: 58%; **b**: 45%; **c**: 55%), **R_2**: 60%; **R_3**:55%).

Scheme 1. Synthesis of *S*-nitrosothiols a–d.

The representations of the molecular structures were plotted in the Gaussview [26] and ChemCraft [27] visualization programs.

We used the method based on the density functional theory (DFT) to investigate the conformational changes, with the help of the functional hybrid B3LYP [28–30] and the standard 6-311+G (2df,2p) basis set. The calculations of orbital interactions were obtained in NBO 3.1 [31].

3. Results and Discussion

3.1. Infrared Spectroscopy Analysis

In the literature we found that the conformational analysis of various 4′-substituted-2-ethylthio-phenylacetate compounds, was performed using IR spectroscopic analysis of the ν_{CO}. Experimental data was supported by B3LYP/6-31G (d,p) and NBO calculations [22]. The computational results predict the presence of three gauche conformers, defined by the orientation of the C—S bond with respect to the carbonyl group, whose intensities and ν_{CO} frequencies are in agreement with the experimental results. NBO analysis suggests that all the conformers are stabilized to the same extent in the gauche conformation via $\sigma_{C-S} \rightarrow \pi^*_{CO}$ and $\pi_{CO} \rightarrow \sigma^*$C—S orbital interactions. The different stability can be attributed to the geometrical arrangement of the C(O)—CH_2—S—CH_2—CH_3. In the present study we applied the same strategy, combining experimental with computational methods.

Table 1 shows the frequencies and relative intensities of the carbonyl stretching bands of the *S*-nitrosothiols 2-methyl-2-(nitrososulfanyl) propyl-phenylacetate-*para*-substituted **R1** (X = H, OMe and Cl), 2-methyl-2-(nitrosothio)-propyl-2-(4-isobutylphenyl)propanoate (derivative of ibuprofen) **R2** and 2-methyl-2-(nitrosothio) propyl-2-(6-methoxynaphthalen-2-yl)propanoate (derivative of naproxen) **R3**. Bands were analytically solved in fundamental transition $\nu_{C=O}$, in solvents of increasing polarity (CCl_4 ε = 2.22; $CHCl_3$ ε = 4.7; and CH_3CN ε = 35.68), and in the first harmonic region in CCl_4.

The matching between the carbonyl profiles in the fundamental and the first overtone region (the latter was measured at the frequency twice that of the fundamental minus two times the mechanical anharmonicity) indicates the existence of any vibrational effect on the fundamental transition of the ν_{CO} mode [32]. Additionally, they presented one single band in the spectrum-mentioned regions, except for the **R1** (X = OMe) compound, which presented two bands, as shown in Figs. 1 and 2 (the analysis of the stretching bands for the other compounds investigated is available in the Supporting information).

Analysis of ν_{CO} in solution determines the different conformations assumed by the compounds [20,21]. The ν_{CO} and the apparent molar absorptivities reported for some thio-estheres, α-(alkylthio)-thioacetates, thiopropionate and thioisobutyrate, indicated the presence of rotamers. These effects were also observed with the SNO-ESTERS analyzed in the present study.

The **R1** (X = Cl) and **R3** compounds (naproxen derivative) presented only one band in all solvents. However, for **R1** (X = H) and **R2** (ibuprofen derivative), two bands with increased polarity appeared, which suggests that a possible conformation could be stabilized in higher polarity solvents, $CHCl_3$ and CH_3CN. The highest-frequency band observed in the spectrum of **R1** (X = OMe) disappeared in more polar solvents ($CHCl_3$ and CH_3CN).

3.2. Theoretical Calculations

A conformational search was performed for the **R1**–**R3** compounds to identify the most stable conformations that they can assume.

In order to guarantee that no degree of freedom of the studied molecules was neglected, we performed a *double scan*, in which the two dihedral angles were taken into account, as they are considered to have the greatest influence on the conformations of this series of compounds in relation to the carbonyl group. We used the Gaussian 09 program to

Table 1
Frequencies (ν, cm^{-1}) and intensity ratios of carbonyl stretching bands in the infrared spectrum for the compounds *S*-nitrosothiols 2-methyl-2-(nitrososulfanyl) propyl-phenylacetate-*para*-substituted **R1** (X = H, OMe and Cl), 2-methyl-2-(nitrosothio)-propyl-2-(4-isobutylphenyl)propanoate (derivative of ibuprofen) **R2** and 2-methyl-2-(nitrosothio)propyl-2-(6-methoxynaphthalen-2-yl)propanoate (derivative of naproxen) **R3**, in solvents of increasing polarity.

Comp.	Y	CCl_4		CCl_4		$CHCl_3$		CH_3CN	
		ν^a_{CO}	P^b	$2\nu^c_{CO}$	P^b	ν^a_{CO}	P^b	ν^a_{CO}	P^b
R1	OMe	1742	78	3463	70	1735	100	1738	100
		1755	22	3484	30	–	–	–	–
	H	–	–	–	–	1703	8	1724	16
		1745	100	3469	100	1736	92	1738	84
	Cl	1748	100	3407	100	1739	100	1742	100
		–	–	–	–	–	–	–	–
R2		–	–	–	–	1720	19	1726	13
		1743	100	3465	100	1734	81	1737	87
R3		1742	100	3464	100	1732	100	1736	100

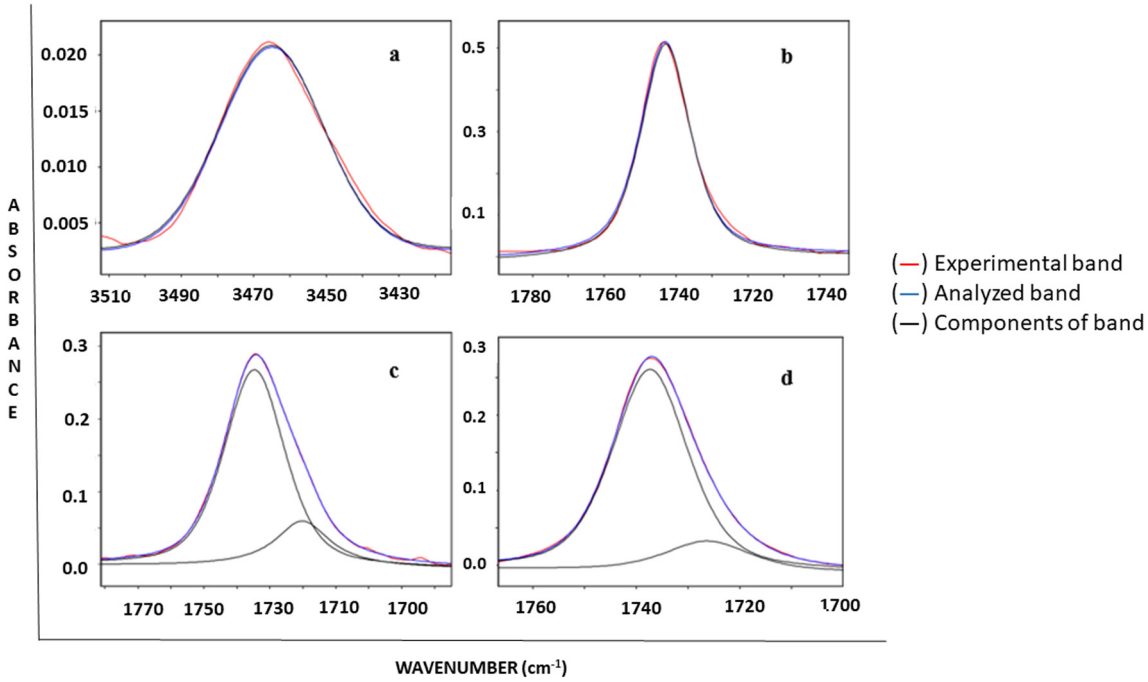

Fig. 1. IR analytically resolved carbonyl stretching bands of 2-(-4-isobutylphenyl) propanoate of 2-methyl-2-(nitrosothiol) propyl **R2**, ibuprofen derivative, in carbon tetrachloride [(a) first overtone and (b) fundamental)], chloroform (c) and acetonitrile (d).

obtain the potential energy surface (PES) graphics related to the energy of the conformer population as a function of the rotational motions employed in the two highlighted dihedral angles (Fig. 3).

The dihedral angles **SC1** = C1—C2—C3—O4 and **SC2** = C3—O5—C6—C7 were increased by steps of 10° until 360°, keeping the **C2**—**C3** and **O5**—**C6** bonds' fixed, using the *semi-empiric* AM1 method [33,34]. This process yielded the surface graphics of the compounds presented in Fig. 4.

The calculations for the minimum global and local conformations in terms of the dihedral angle α = C1—C2—C3—O4 (Fig. 5) disclosed one preferential conformation for all the studied compounds **R1**–**R3**. Several surface geometries were selected and all were found to converge to this conformation in relation to α, and there was no significant change for any other angle.

The geometry data (the relative Gibbs free energy, relative populations, dipole moments, carbonyl and nitroso stretching frequencies, and dihedral angles) at the B3LYP/6-311+G (2df,2dp) level of theory are reported in Table 2 and Fig. 6 and are taken as representatives for the whole series of compounds. The calculation results for compounds R1–R3 suggest the presence of one stable *anti-clinal* (*ac*) conformer in vacuum, with α dihedral angle (O═C—C—Ar) varying between 83 and 85°.

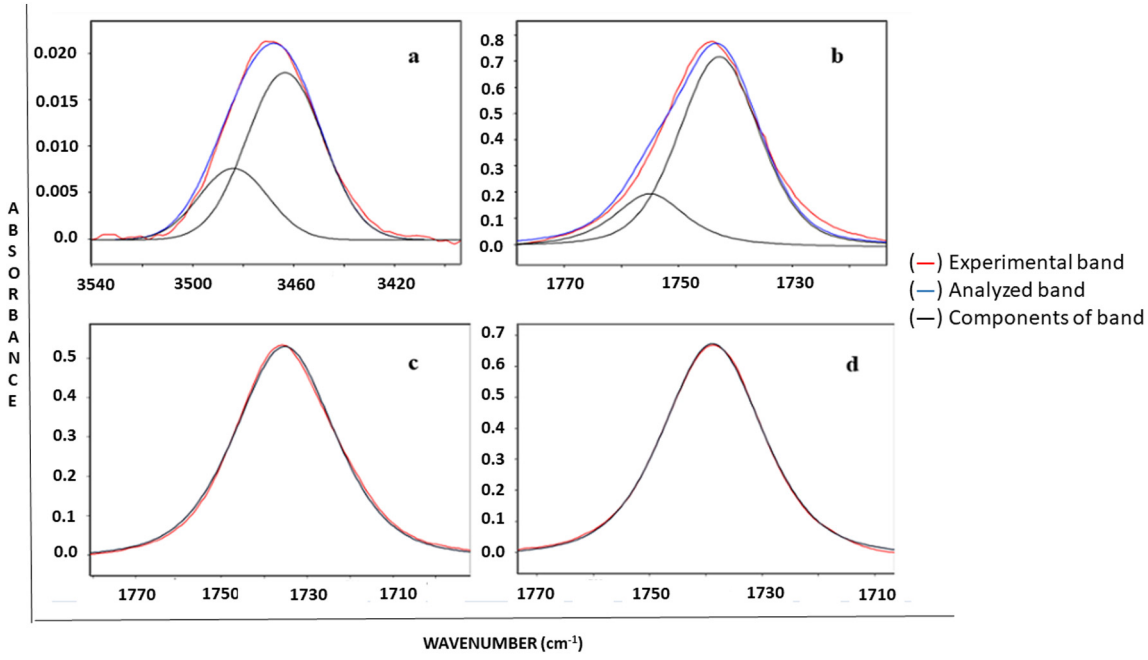

Fig. 2. IR analytically resolved carbonyl stretching bands of 2-(4-methoxyphenylacetate) of 2-methyl-2-(nitrosothiol) propyl **R1** (X = OMe) in carbon tetrachloride [(a) first overtone and (b) fundamental)], chloroform (c) and acetonitrile (d).

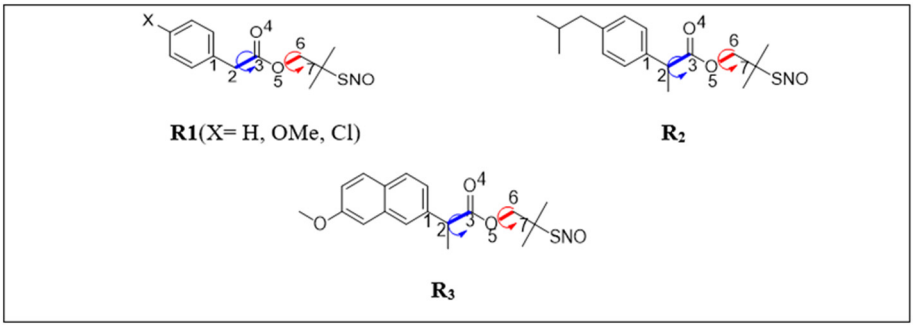

Fig. 3. Selected dihedral angles in conformational search, **SC1** = C1—C2—C3—O4 and **SC2** = C3—O5—C6—C7 in relation to carbonyl group, for the **R1**–**R3** compounds.

The geometry data obtained through the theoretical calculations agreed with the experimental results obtained from the IR spectra in CCl_4 for all the compounds. One carbonyl stretching band was observed for all the studied compounds, except for the $\mathbf{R_1}$ (X = OMe) compound, which had two bands, both in the fundamental and the first harmonic region.

Table 3 displays the atomic charge values, positive and negative, for each atom and Table 4 shows the relevant interatomic distances and the sum of the corresponding van der Waals radii.

On examining the data presented in Tables 3 and 4 regarding the stable conformers for **R1** (X = H, OMe, and Cl), **R2**, and **R3**, we noticed the occurrence of 4–5 electrostatic and charge transfer (intramolecular hydrogen bonds) interactions between the negative oxygen atoms in the carbonyl and the ester groups, and the adjacent hydrogen atoms responsible for the stability of these conformations. The intramolecular hydrogen bonds are shown in Fig. 7.

Since all the compounds converged towards one single stable conformation with *ac* geometry in relation to the α dihedral, we calculated the preferential conformation for the R—SNO group by running a single scan (in AM1) around the dihedral angle C(1)—S(2)—N(3)═O(4). The starting geometries used were the ones found for the global minimums of the **R1**–**R3** compounds in relation to the carbonyl group, rotating the

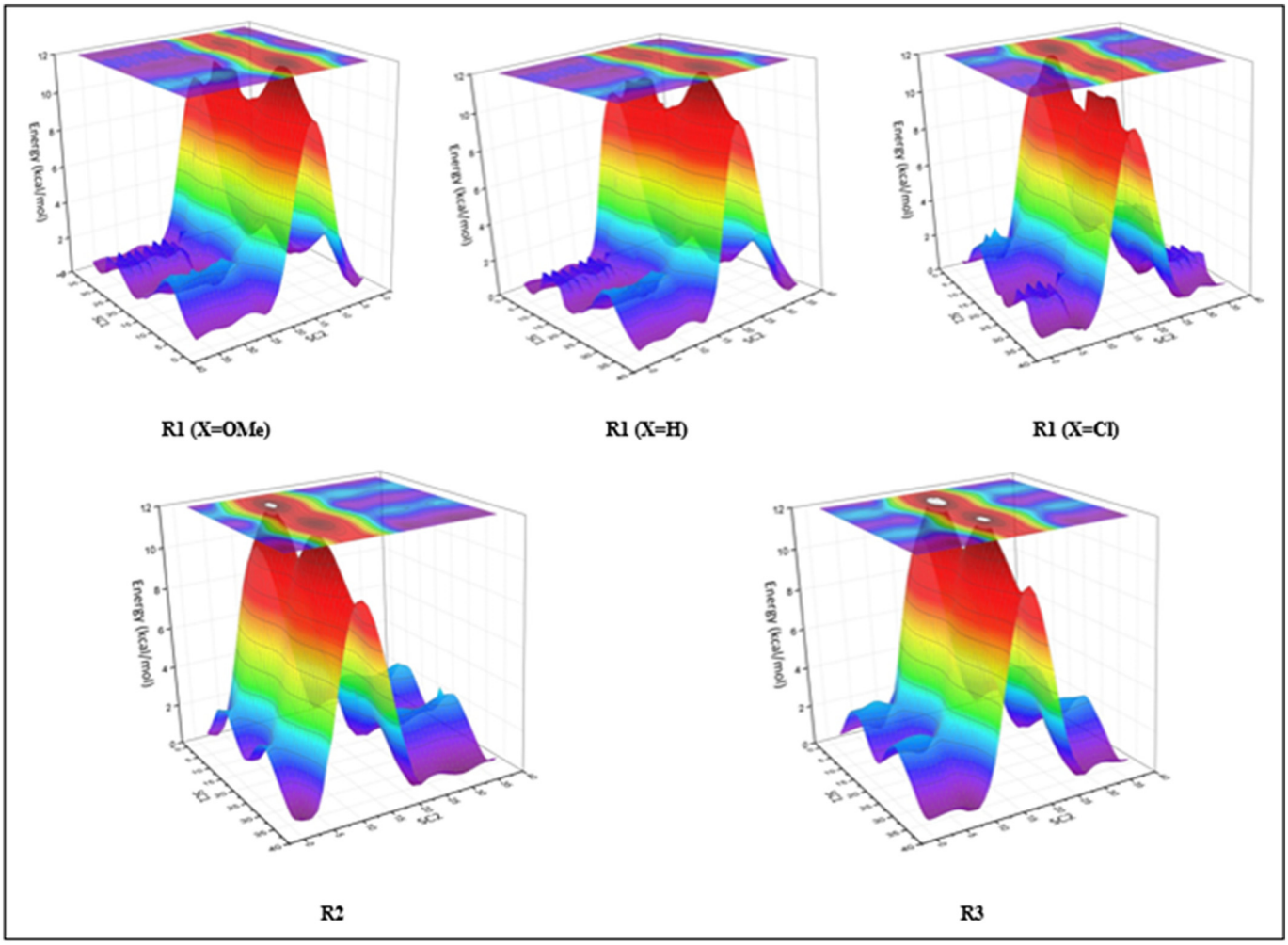

Fig. 4. Energy surface graphics as a function of the rotation of SC1 = C1—C2—C3—O4 and SC2 = C3—O5—C6—C7 dihedral angles, optimized at AM1 semi-empirical level, for the **R1**–**R3** compounds.

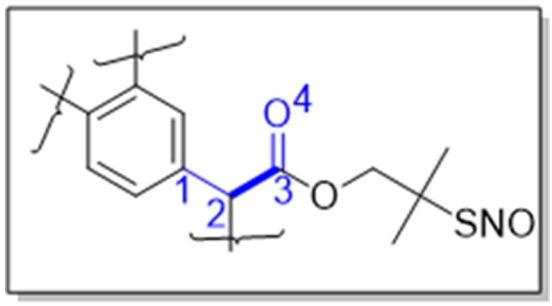

Fig. 5. The α = C1—C2—C3—O4 dihedral angle.

angle through steps of 10° until 360°, keeping the S2—N3 bond fixed (Fig. 8). All the compounds presented the same behavior, yielding a graph of energy as a function of rotation.

Fig. 9 shows the plot of energy as a function of the dihedral angle selected for the **R1** (X = OMe) compound. The minima had their geometry optimized using DFT calculations using the B3LYP hybrid functional and the set of *standard* 6-311+G (2df, 2p) basis set. These findings are presented in Table 5. There were no significant changes in the values of the dihedral angles obtained in relation to the values presented in Table 2.

As described previously [35], the S—NO bond has a significant double-bond character owing to the delocalization of the sulfur atom electron pair in the nitroso group. This produces two possible conformations, *syn* (*cis*) and *anti* (*trans*), which may not directly interfere in the carbonyl bond stretching due to the distance from the S—NO group. Thus, it is possible to observe a conformational equilibrium between *syn* (*cis*) and *anti* (*trans*) conformations with different populations, without any direct influence on the carbonyl bond stretching.

Nevertheless, for all the **R1**–**R3** compounds, we found that the R—S—NO group tended to assume the *trans* (*anti*) conformation, with an energy difference of ~5 kcal·mol^{-1} compared to the *cis* (*syn*) conformation.

In contrast to previous statements, the ratio between the *cis* (*syn*) and the *trans* (*anti*) conformers is not directly related to the steric effect of the methyl groups on the carbon-α, [3,6] but this ratio results from the balance of opposing interactions in the *cis* (*syn*) conformation, namely, the repulsive interaction between the sulfur and the nitrogen lone pairs and the stabilizing contribution of a C(α)—H···O hydrogen bond.

This theoretical approach entirely relies on the analysis of the electron density and its corresponding reduced gradient, and it was already successfully used to detect both intra- and intermolecular interactions. These interactions correspond to low-value peaks of the reduced density gradient occurring at low values of the electron density, and they can be visualized in real space plotting proper low-value reduced gradient isosurfaces [36].

In our study, the values found in the theoretical calculations for the size of S—N bonds for the **R1**–**R3** compounds, ranging from 1.62 to 1.82 Å, are showed in Table 4. The reliability and accuracy of the DFT methods to obtain optimized structures and the homolytic breakdown energy of S—N bonds to yield NO of a range of *S*-nitrosothiols, has been investigated. Among all methods considered, optimized S—N bond lengths are found to be highly dependent on the basis set being employed. In general, it has been found that the length of the S—N bond ranging from 1.8 to 1.9 A were stabilized for the hyper conjugative interactions [37].

Interestingly, were reported the high-resolution crystal structure determination of an *S*-nitroso-cysteine derivative. Given the importance of *S*-nitrosation of cysteine residues in biology, the knowledge of the solid-state conformations of the *S*-nitroso-L-cysteine group allow for more complete predictions of the conformations of *S*-nitroso-L-cysteinyl groups in nitrosated peptides and biomolecules. [38] Were observed the S—N bond lengths of the major occupancy rotamer of 1.745–1.781 Å range [39].

Our findings are in agreement with those described by Meyer et al. [37] and we can suggest that hyper conjugative interactions may explain the relative stability of the **R1**–**R3** compounds. Nevertheless, the relative stability of the **R1**–**R3** compounds does not preclude their ability as potential NO donors.

The most stable *trans* (*anti*) conformations of **R1**–**R3** were then subjected to the NBO calculation and Tables 6 and 7 presents all the orbital interactions with energy above 2 kcal·mol^{-1}. The highest energy value of the orbital interactions for the compounds of the **R1**–**R3** series referred to the aromatic ring. However, these values were not listed because high values for these interactions were expected.

The *ac* conformers of the **R1**–**R3** compounds were stabilized to about the same extent by the strong $n_{O(COC)} \rightarrow \pi^*_{(CO)}$ and $n_{O(co)} \rightarrow \sigma^*_{(C-O)}$ interactions (ca. 47 kcal·mol^{-1} and 35 kcal·mol^{-1}, respectively) as a consequence of the suitable symmetry exhibited by the oxygens lone pairs of the carbonyl and ester groups.

Work of Khomyakov and Timerghazin reported accurate ab initio calculations of the structure and properties of *S*-nitrosothiols. [40] It is interesting to consider that exist a relation between the antagonistic

Table 2
Relative free energy (kcal mol^{-1}), relative population (%), calculated stretching band ($\nu_{C=O}$ and $\nu_{N=O}$, cm^{-1}), dipole moment (μ/D), and selected dihedral angles (deg) for the different conformers of *para*-substituted 2-methyl-2-(nitrosothiol)propyl-phenylacetates *para*-substituted **R1** (X = H, OMe, and Cl), and the derivatives of ibuprofen **R2** and naproxen **R3**, at the DFT-B3LYP/6-311+G (2df,2p) level of theory.

Comp.	X	Conf.	E[a]	P[b]	$\nu_{C=O}$	$\nu_{N=O}$	μ/D	Dihedral angles/°[c]										
								α	β	γ	δ	ε	ϕ	ω	φ	Ψ	α′	β′
R1	OMe	*ac*	0	100	1790	1635	4.12	94.84	−84.02	178.08	−116.19	0.90	−59.90	65.09	102.37	179.94	–	–
	H	*ac*	0	100	1792	1636	3.84	−93.32	85.62	−177.88	121.46	1.08	60.30	−64.74	177.81	179.93	–	–
	Cl	*ac*	0	100	1788	1639	2.86	96.17	−82.63	177.70	172.72	1.19	−61.05	64.02	−178.48	179.78	–	–
R2		*ac*	0	100	1786	1628	3.92	93.93	−84.99	177.94	−117.01	1.00	−58.58	66.12	179.95	179.96	30.95	150.11
R3		*ac*	0	100	1784	1635	4.71	95.28	−83.53	176.66	−175.39	−2.18	−61.91	63.10	−179.38	178.92	−29.51	151.66

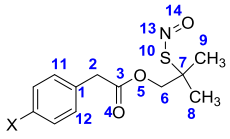

R1 (X= CH_3O, H, Cl)

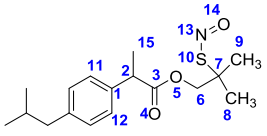

R2

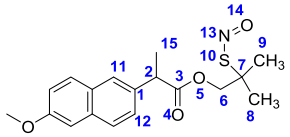

R3

[a] The relative free Gibbs energy (relative electronic energy plus ZPE correction).
[b] The relative population is reported as a percentage.
[c] α = C(1)—C(2)—C(3)—O(4); β = C(1)—C(2)—C(3)—O(5); γ = C(2)—C(3)—O(5)—C(6); δ = C(3)—O(5)—C(6)—C(7); ε = O(4)—C(3)—O(5)—C(6); ϕ = O(5)—C(6)—C(7)—C(8); ω = O(5)—C(6)—C(7)—C(9); φ = O(5)—C(6)—C(7)—S(10); Ψ = C(7)—S(10)—N(13)—O(14); α′ = C(15)—C(2)—C(3)—O(4); β′ = C(15)—C(2)—C(3)—O(5).

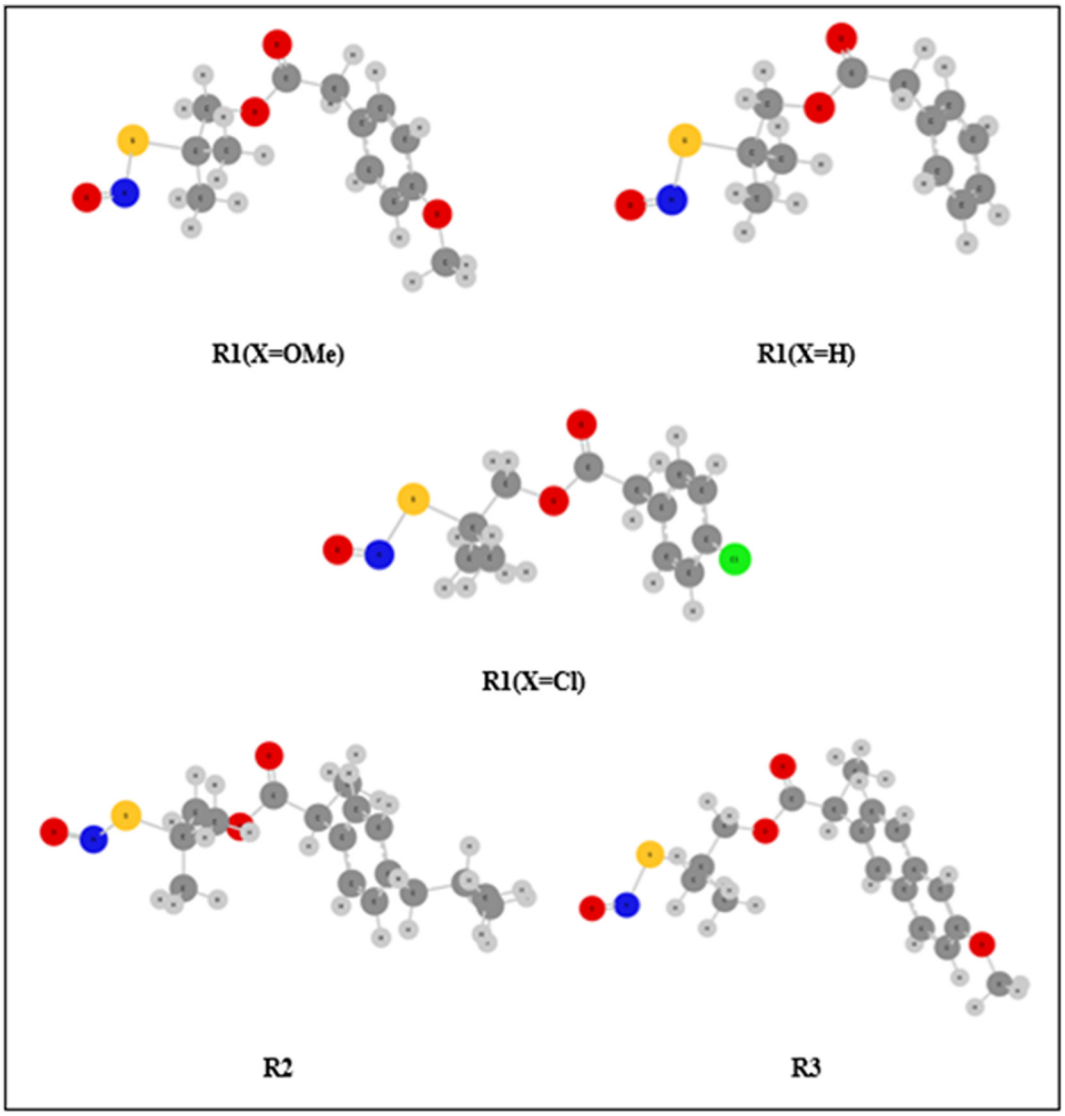

Fig. 6. Optimized geometric representation, at B3LYP/6-311+G(2df,2p) level, for *ac* conformers of the **R1**–**R3** compounds.

nature and the multireference character of the R—SNO group. The calculated S—N bond length in the *cis-trans* interconversion shows as the S—N bond loses its double-bond character, to support the hypothesis that connects the ionic component RS^{-}/NO^{+} and the multi-reference character of the R—SNO group. Since the unusual electronic structure of the R—SNO group likely plays a defining role in the biological reactivity of *S*-nitrosothiols, further investigations in this direction are warranted.

Controversies remain on the nature of the S—N bonds in RSNO compounds. On one hand, quite high rotation barriers were observed for the *syn/anti* interconversion, suggesting a partial S—N double-bond character [41]. On the other hand, the computed homolytic dissociation

Table 3
Charge of Muliken (e) of selected atoms obtained at DFT-B3LYP/6-311+G (2df,2p) level for the 2-methyl-2-(nitrosothiol)propyl-phenylacetates-*para*-substituted **R1** (X = H, OMe and Cl), and the derivatives of ibuprofen **R2** and naproxen **R3** (the minus sign indicates excess of negative charge).

Comp.	X	Conf.	C1	C2	C3	O4	O5	C6	C7	S	N	O
R1	OMe	*ac*	0.70	−0.141	0.14	−0.34	−0.05	−0.20	1.16	−0.319	−0.11	0.02
	H	*ac*	0.86	−0.26	0.13	−0.34	−0.05	−0.22	1.11	−0.33	0.12	0.022
	Cl	*ac*	0.49	−0.28	0.11	−0.33	−0.05	−0.336	1.05	−034	−0.11	0.02
R2		*ac*	0.49	0.50	0.55	−0.16	−0.03	−0.33	−0.47	1.15	−0.26	0.02
R3		*ac*	0.39	0.63	−0.27	−0.32	−0.03	−0.28	1.08	−0.34	−0.11	0.02

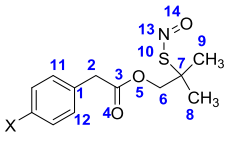

R1 (X= CH_3O, H, Cl)

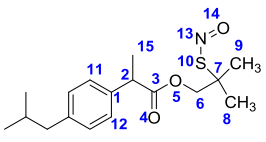

R2

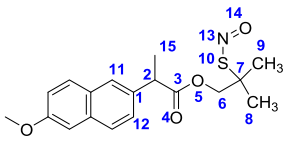

R3

Table 4
Selected interatomic distances (Å) (intramolecular hydrogen bonds) and r(S—N) bond (Å) at DFT-B3LYP/6-311+G(2df,2p) level of 2-methyl-2-(nitrosothiol)propyl-phenylacetates-*para*-substituted **R1** (X = H, OMe and Cl) and the derivatives of ibuprofen **R2** and naproxen **R3** (sum of van der Waals radii O···H = 2.72 Å).

Comp.	X	Conf.	Interatomic Distances (Å)							r(S-N)
			O_4...H_2	O_4...H_6	O_4...H_{11}	O_4...H_{12}	O_5...H_2	O_5...H_8	O_5...H_9	
R1	**OMe**	*ac*	2.56	2.26	-	3.10	2.47	2.62	2.70	1.74
	H	*ac*	2.56	2.25	-	3.11	2.47	2.62	2.68	1.84
	Cl	*ac*	2.56	2.56/2.69	-	3.07	2.49	2.61	2.59	1.73
R2		*ac*)	3.20	2.26	2.85	4.87	2.40	2.61	2.70	1.82
R3		*ac*	3.20	2.58/2.67	2.81	4.92	2.42	2.59	2.60	1.62

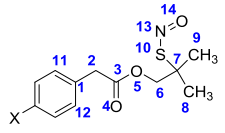

R1 (X= CH_3O, H, Cl)

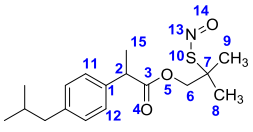

R2

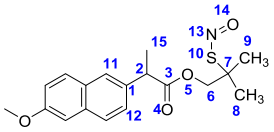

R3

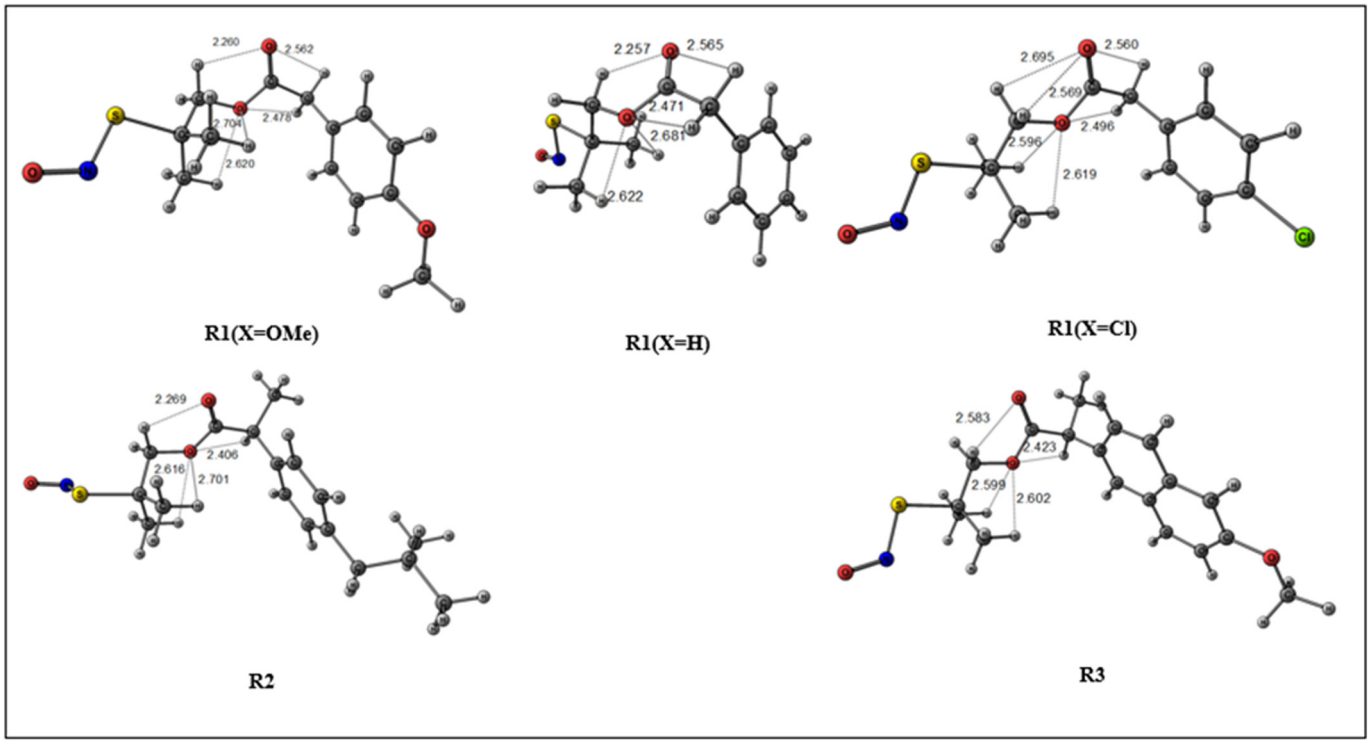

Fig. 7. Molecular graphs for the *ac* conformers of the compounds **R1**–**R3**, showing electrostatic and charge transfer (intramolecular hydrogen bonds) interactions between the negative oxygen atoms in the carbonyl and the ester groups and the adjacent hydrogen atoms.

energy, typically 30 kcal mol^{-1}, suggested that this bond is relatively weak. This fact may be related with its photo degradation and also with the formation of NO by products. Although it is commonly accepted that *S*-nitrosothiols decompose under formation of the corresponding disulfides and NO by a unimolecular hemolytic scission of the S—N bond [41].

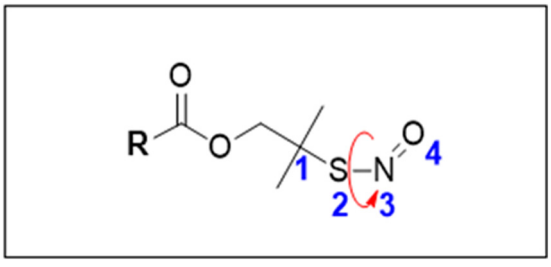

Fig. 8. Selected dihedral angles in the conformational search of the preferential conformation of the *S*-nitrosothiol group C(1)—S(2)—N(3)═O(4).

The NBO results also revealed that the $n_{O(NO)} \rightarrow \sigma^*_{(S-N)}$ hyper conjugative interaction (40–44 kcal·mol^{-1}) is quite effective, weakening the σ bond and resulting in an increase of S—N bond length in the *S*-nitrosothiol derivatives. The strong $n_S \rightarrow \pi^*_{(NO)}$ delocalization (20–-28 kcal·mol^{-1}), induces a partial π character to the S—N bond. The weak σ_{S-N} bond indicates strong delocalization of the electron pair in $O_{(NO)}$ due to the $n_{O(NO)} \rightarrow \sigma^*_{(S-N)}$ interaction, responsible for the elongation of the S—N bond, which in turn increases the capacity of NO release by the compounds **R1**–**R3**. The $n_{O(NO)} \rightarrow \sigma^*_{(S-N)}$ hyper conjugative interaction calculated for the **R1** (X = OMe) compound is presented in Fig. 10.

The photoelectron spectrum of a thionitrite species in the gas phase was measured and interpreted with the help of electron propagator calculations at the OVGF/6-311+G(2df) level of approximation. The electronic structure in the valence region of $(CH3)_3CSNO$ was

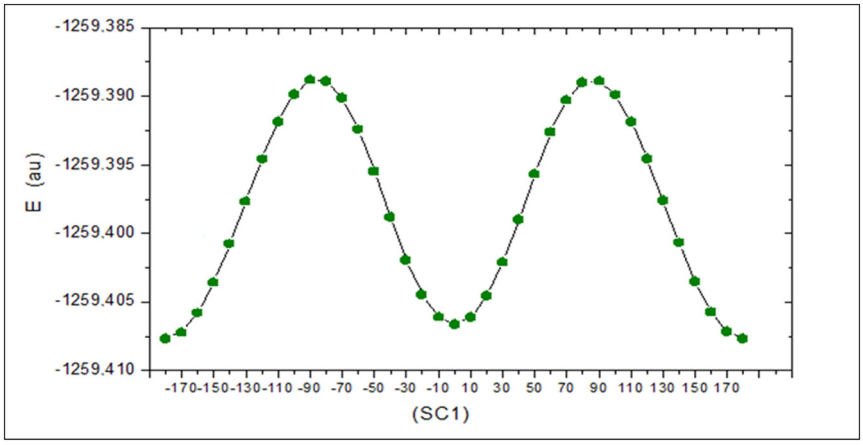

Fig. 9. Energy surface graphics as a function of the rotation of C(1)–S(2)–N(3)=O(4) dihedral angles of the **R1** (X = OMe) compound.

characterized by ionizations of electrons formally located at the thionitrite moiety [42]. The energy bands observed in the spectrum were associated with ionization processes from the outermost $n\pi_{(S)}$ (HOMO), $n_{(O)}$ and $\pi_{(N=O)}$ orbitals, respectively. The S 2p absorption spectra is explained in terms of different LUMO orbitals, namely $\sigma^*_{(S-N)}$ and $\pi^*_{(NO)}$.

The biological and potential pharmacological activities of *S*-nitrosothiols are not circumscribed to their capacity to release NO. *S*-Nitrosothiols may decompose to form NO^- which under certain conditions, generate peroxynitrite-$ONOO^-$ and nitrous acid–HNO_2 (reviewed in [43]). Another important aspect of the complex chemistry of *S*-nitrosothiols is their capacity to transfer nitrosonium–NO^+ to cellular thiols, in a process known as transnitrosation [44]. The transnitrosation reactions of **R1**–**R3** SNO-ESTERS are currently under investigation in our laboratory.

4. Conclusion

We have examined the relationship between the structure and stability of the **R1**–**R3** SNO-ESTERS. A thorough study of their conformational preferences showed that, the *trans* (*anti*) conformers of the S—NO bond are prevalent for all compounds studied.

Combined analysis of experimental and theoretical data demonstrated that **R1**–**R3** *S*-nitrosothiols showed a preferential *anti-clinal* conformation in relation to the carbonyl group.

The NBO analysis showed that the $n_{O(NO)} \rightarrow \sigma^*_{(S-N)}$ hyper conjugative interaction is quite effective in weakening the σ bond, which leads to an increase in the S—N bond length in *S*-nitrosothiols. The strong $n_S \rightarrow \pi^*_{(NO)}$ delocalization induces a partial π character to the S—N bond. The $n_{O(NO)} \rightarrow \sigma^*_{(S-N)}$ interaction, responsible for the elongation of the S—N bond, increases the capacity of NO release by all the **R1**–**R3** compounds.

The main goal of the present study was to get insights into the SNO-ESTERS structure, stability, reactivity, and their capacity to release NO. Such information will lead us to propose the synthesis of new SNO-ESTERS characterized by enhanced anti-inflammatory actions without the well characterized harmful side effects. In particular, we believe that a detailed analysis of inter- and intra-molecular interactions in which the different *S*-nitrosothiols are involved will be of fundamental importance to propose suitable pharmacophore descriptors that will drive the design of new potential drugs.

Conflict of Interest

All authors declare no conflict of interest.

Acknowledgments

The authors thank Fundação de Amparo à Pesquisa do Estado de São Paulo (FAPESP - Grant Numbers: 2010/51784-3 and 2013/16644-4) for financial support. The authors also thank Coordenação Nacional de Aperfeiçoamento do Ensino Superior (CAPES - Brazil) for the research fellowships granted to M.M.R. and D.R.P. Professor Paulo Roberto Olivato is gratefully acknowledged for providing laboratory facilities.

Table 5
Calculated and experimental stretching ($\nu_{N=O}$, cm^{-1}), dipole moment (μ/D) and selected dihedral angles (deg) for *trans* conformers, in relation to C—S—N—O (Ψ) dihedral angle rotation, of the *anti clinal* conformer most stable for 2-methyl-2-(nitrosothiol)propyl-phenylacetates-*para*-substituted **R1** (X = H, OMe and Cl) and the derivatives of ibuprofen **R2** and naproxen **R3**, at the DFT-B3LYP/6-311+G (2df,2p) level of theory.

Comp.	X	Conf.	$\nu_{N=O}$ (calc.)	$\nu_{N=O}$ (exp,)	μ/D	α	β	Dihedral Angles /° [a]								
								γ	δ	ε	ϕ	ω	φ	Ψ	α'	β'
R1	**OMe**	*trans*	1635	1637	4.12	94.84	-84.02	178.08	-116.19	0.90	-59.90	65.09	102.37	179.94	-	-
	H	*trans*	1636	1635	3.84	-93.32	85.62	-177.88	121.46	1.08	60.30	-64.74	177.81	179.93		
	Cl	*trans*	1639	1636	2.86	96.17	-82.63	177.70	172.72	1.19	-61.05	64.02	-178.48	179.78		
R2		*trans*	1628	1634	3.92	93.93	-84.99	177.94	-117.01	1.00	-58.58	66.12	179.95	179.96	30.95	150.11
R3		*trans*	1635	1632	4.71	95.28	-83.53	176.66	-175.39	-2.18	-61.91	63.10	-179.38	178.92	-29.51	151.66

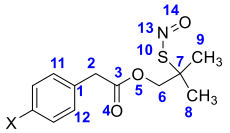

R1 (X= CH_3O, H, Cl)

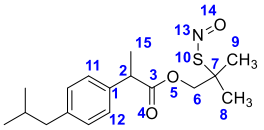

R2

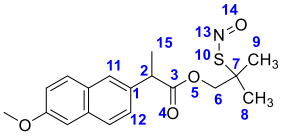

R3

[a] α = C(1)–C(2)–C(3)–O(4); β = C(1)–C(2)–C(3)–O(5); γ = C(2)–C(3)–O(5)–C(6); δ = C(3)–O(5)–C(6)–C(7); ε = O(4)–C(3)–O(5)–C(6); ϕ = O(5)–C(6)–C(7)–C(8); ω = O(5)–C(6)–C(7)–C(9); φ = O(5)–C(6)–C(7)–S(10); Ψ = C(7)–S(10)–N(13)–O(14); α′ = C(15)–C(2)–C(3)–O(4); β′ = C(15)–C(2)–C(3)–O(5).

Table 6
Energy of electronic interactions calculated by the Natural Bond Orbital method (kcal·mol^{-1}), for the *para*-substituted 2-methyl-2-(nitrosothiol)propyl-phenylacetates **R1** (X = H, OMe and Cl).

X=OMe		X=H		X=Cl	
Interaction	E	Interaction sOrbitalares	E	Interaction	E
$\sigma_{C(3)-C(11)}\rightarrow\pi^*_{C(14)-O(15)}$	3.29	$\pi_{C(3)-C(4)}\rightarrow\sigma^*_{C(12)-O(15)}$	3.32	$\sigma_{C(11)-H(12)}\rightarrow\sigma^*_{C(14)-O(16)}$	3.84
$\sigma_{C(4)-C(5)}\rightarrow\sigma^*_{C(3)-C(11)}$	3.64	$\sigma_{C(3)-C(12)}\rightarrow\pi^*_{C(15)-O(16)}$	3.32	$\sigma_{C(11)-H(13)}\rightarrow\sigma^*_{C(3)-C(4)}$	4.12
$\pi_{C(11)-H(12)}\rightarrow\pi^*_{C(14)-O(16)}$	3.86	$\sigma_{C(3)-H(13)}\rightarrow\sigma^*_{C(15)-O(16)}$	3.63	$\sigma_{C(11)-H(13)}\rightarrow\sigma^*_{C(14)-O(15)}$	3.54
$\pi_{C(11)-H(13)}\rightarrow\pi^*_{C(14)-O(15)}$	3.56	$\sigma_{C(3)-H(13)}\rightarrow\pi^*_{C(15)-O(16)}$	2.37	$\sigma_{C(11)-H(13)}\rightarrow\pi^*_{C(14)-O(15)}$	2.40
$\sigma_{C(11)-C(14)}\rightarrow\sigma^*_{O(16)-C(17)}$	4.20	$\sigma_{C(12)-H(14)}\rightarrow\pi^*_{C(3)-C(4)}$	2.12	$\sigma_{C(11)-C(14)}\rightarrow\pi^*_{C(2)-C(3)}$	2.34
$\sigma_{O(16)-C(17)}\rightarrow\sigma^*_{C(11)-C(14)}$	2.12	$\sigma_{C(12)-H(14)}\rightarrow\sigma^*_{C(15)-O(17)}$	3.73	$\sigma_{C(11)-C(14)}\rightarrow\sigma^*_{O(16)-C(18)}$	4.12
$\sigma_{C(20)-S(34)}\rightarrow\sigma^*_{O(16)-C(17)}$	4.79	$\sigma_{C(12)-C(15)}\rightarrow\pi^*_{C(3)-C(4)}$	2.47	$\sigma_{O(16)-C(18)}\rightarrow\sigma^*_{C(11)-C(14)}$	2.33
$\sigma_{C(21)-H(22)}\rightarrow\sigma^*_{C(20)-C(25)}$	3.82	$\sigma_{C(12)-C(15)}\rightarrow\sigma^*_{O(17)-C(18)}$	4.21	$\sigma_{O(16)-C(18)}\rightarrow\sigma^*_{C(21)-S(30}$	2.16
$\sigma_{C(21)-H(23)}\rightarrow\sigma^*_{C(20)-S(34)}$	5.62	$\sigma_{C(21)-S(30)}\rightarrow\sigma^*_{C(22)-H(23)}$	2.45	$\sigma_{O(16)-H(19)}\rightarrow\sigma^*_{C(21)-C(26)}$	3.67
$\sigma_{C(21)-H(24)}\rightarrow\sigma^*_{C(17)-C(20)}$	3.76	$\sigma_{C(21)-S(30)}\rightarrow\sigma^*_{C(26)-H(29)}$	2.45	$\sigma_{C(21)-S(30)}\rightarrow\sigma^*_{O(16)-C(18)}$	4.77
$\sigma_{C(25)-H(28)}\rightarrow\sigma^*_{C(20)-S(34)}$	5.63	$\sigma_{C(22)-H(23)}\rightarrow\sigma^*_{C(21)-S(30)}$	5.62	$\sigma_{C(21)-S(30)}\rightarrow\sigma^*_{C(22)-H(24)}$	2.43
$\eta_{1\ O(15)}\rightarrow\sigma^*_{C(11)-C(14)}$	2.34	$\sigma_{C(22)-H(25)}\rightarrow\sigma^*_{C(21)-C(26)}$	3.86	$\sigma_{C(21)-S(30)}\rightarrow\sigma^*_{C(26)-H(29)}$	2.45
$\eta_{2\ O(15)}\rightarrow\sigma^*_{C(11)-C(14)}$	18.56	$\sigma_{C(26)-H(27)}\rightarrow\sigma^*_{C(21)-C(22)}$	3.83	$\sigma_{C(22)-H(23)}\rightarrow\sigma^*_{C(18)-C(21)}$	3.80
$\eta_{2\ O(15)}\rightarrow\sigma^*_{C(14)-O(16)}$	35.42	$\sigma_{C(26)-H(28)}\rightarrow\sigma^*_{C(18)-C(21)}$	3.77	$\sigma_{C(22)-H(24)}\rightarrow\sigma^*_{C(21)-S(30)}$	5.62
$\eta_{1\ O(16)}\rightarrow\sigma^*_{C(14)-O(15)}$	8.36	$\sigma_{C(26)-H(29)}\rightarrow\sigma^*_{C(21)-S(30)}$	5.60	$\sigma_{C(26)-H(29)}\rightarrow\sigma^*_{C(21)-S(30)}$	5.56
$\eta_{2\ O(16)}\rightarrow\pi^*_{C(14)-O(15)}$	47.06	$\eta_{1\ O(16)}\rightarrow\sigma^*_{C(12)-C(15)}$	2.32	$\eta_{1\ O(15)}\rightarrow\sigma^*_{C(11)-C(14)}$	2.36
$\eta_{2\ O(16)}\rightarrow\sigma^*_{C(17)-C(20)}$	3.60	$\eta_{2\ O(16)}\rightarrow\sigma^*_{C(12)-C(15)}$	18.69	$\eta_{2\ O(15)}\rightarrow\sigma^*_{C(11)-C(14)}$	18.85
$\eta_{2\ S(34)}\rightarrow\sigma^*_{C(20)-C(25)}$	3.00	$\eta_{2\ O(16)}\rightarrow\sigma^*_{C(15)-O(17)}$	35.74	$\eta_{2\ O(15)}\rightarrow\sigma^*_{C(14)-O(16)}$	35.18
$\eta_{2\ S(34)}\rightarrow\pi^*_{N(35)-O(36)}$	28.63	$\eta_{1\ O(17)}\rightarrow\sigma^*_{C(18)-H(20)}$	2.75	$\eta_{1\ O(16)}\rightarrow\sigma^*_{C(14)-O(15)}$	7.80
$\eta_{2O(36)}\rightarrow\sigma^*_{S(34)-O(N35)}$	43.40	$\eta_{2\ O(17)}\rightarrow\pi^*_{C(15)-O(16)}$	47.42	$\eta_{2\ O(16)}\rightarrow\pi^*_{C(14)-O(15)}$	48.86
		$\eta_{2\ O(17)}\rightarrow\sigma^*_{C(18)-H(19)}$	4.01	$\eta_{2\ O(16)}\rightarrow\sigma^*_{C(18)-H(19)}$	4.15
		$\eta_{2\ S(30)}\rightarrow\sigma^*_{C(21)-C(22)}$	3.00	$\eta_{2\ S(30)}\rightarrow\sigma^*_{C(21)-C(22)}$	2.98
		$\eta_{2\ S(30)}\rightarrow\sigma^*_{N(31)-O(32)}$	28.21	$\eta_{2\ S(30)}\rightarrow\sigma^*_{C(21)-C(26)}$	2.97
		$\eta_{2\ O(32)}\rightarrow\sigma^*_{S(30)-N(31)}$	43.60	$\eta_{2\ S(30)}\rightarrow\sigma^*_{N(31)-O(32)}$	20.61
				$\eta_{2\ O(32)}\rightarrow\sigma^*_{S(30)-N(41)}$	44.06
Σ	**234.66**	**Σ**	**238.49**	**Σ**	**230.97**

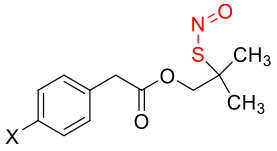

R1 (X= CH_3O, H, Cl)

Table 7
Energy of electronic interactions calculated by the Natural Bond Orbital method (kcal·mol^{-1}), for the derivatives of ibuprofen **R2** and naproxen **R3**.

R2		R3	
Interaction	E	Interaction	E
$\sigma_{C(3)-C(11)}\rightarrow\sigma^*_{C(13)-O(14)}$	3.05	$\sigma_{C(13)-C(17)}\rightarrow\pi^*_{C(23)-O(25)}$	3.24
$\sigma_{C(11)-H(12)}\rightarrow\sigma^*_{C(13)-O(14)}$	3.69	$\sigma_{C(14)-H(16)}\rightarrow\sigma^*_{C(10)-C(13)}$	4.01
$\sigma_{C(11)-H(12)}\rightarrow\pi^*_{C(13)-O(14)}$	2.74	$\sigma_{C(17)-H(18)}\rightarrow\sigma^*_{C(13)-C(14)}$	4.63
$\sigma_{C(11)-H(12)}\rightarrow\sigma^*_{C(16)-H(18)}$	2.61	$\sigma_{C(17)-H(18)}\rightarrow\sigma^*_{C(23)-O(25)}$	3.67
$\sigma_{C(16)-H(17)}\rightarrow\sigma^*_{C(3)-C(11)}$	3.20	$\sigma_{O(24)-C(31)}\rightarrow\sigma^*_{C(17)-C(23)}$	2.21
$\sigma_{C(33)-H(34)}\rightarrow\sigma^*_{C(36)-C(41)}$	3.76	$\sigma_{C(27)-H(28)}\rightarrow\sigma^*_{C(1)-O(26)}$	3.51
$\sigma_{C(33)-H(35)}\rightarrow\sigma^*_{C(36)-C(37)}$	3.70	$\sigma_{C(34)-S(43)}\rightarrow\sigma^*_{O(24)-C(31)}$	4.68
$\sigma_{C(36)-S(45)}\rightarrow\sigma^*_{O(15)-C(33)}$	4.06	$\sigma_{C(34)-S(43)}\rightarrow\sigma^*_{C(35)-H(37)}$	2.25
$\sigma_{C(36)-S(45)}\rightarrow\sigma^*_{C(37)-H(48)}$	2.35	$\sigma_{C(35)-H(37)}\rightarrow\sigma^*_{C(34)-S(43)}$	5.57
$\sigma_{C(36)-S(45)}\rightarrow\sigma^*_{C(41)-H(42)}$	2.86	$\sigma_{C(35)-H(38)}\rightarrow\sigma^*_{C(31)-C(34)}$	3.78
$\sigma_{C(37)-H(38)}\rightarrow\sigma^*_{C(36)-S(45)}$	5.69	$\sigma_{C(39)-H(40)}\rightarrow\sigma^*_{C(34)-C(35)}$	3.88
$\sigma_{C(37)-H(39)}\rightarrow\sigma^*_{C(33)-C(36)}$	3.79	$\sigma_{C(39)-H(41)}\rightarrow\sigma^*_{C(31)-C(34)}$	3.78
$\sigma_{C(37)-H(40)}\rightarrow\sigma^*_{C(36)-C(41)}$	3.80	$\sigma_{C(39)-H(42)}\rightarrow\sigma^*_{C(34)-S(43)}$	5.62
$\sigma_{C(41)-H(42)}\rightarrow\sigma^*_{C(36)-S(45)}$	4.68	$\eta_{1\ O(24)}\rightarrow\sigma^*_{C(23)-O(25)}$	7.79
$\sigma_{C(41)-H(43)}\rightarrow\sigma^*_{C(36)-C(47)}$	3.64	$\eta_{2\ O(24)}\rightarrow\pi^*_{C(23)-O(25)}$	47.05
$\sigma_{C(41)-H(43)}\rightarrow\sigma^*_{C(33)-C(36)}$	3.61	$\eta_{2\ O(24)}\rightarrow\sigma^*_{C(31)-H(32)}$	4.31
$\eta_{2\ O(14)}\rightarrow\sigma^*_{C(11)-C(13)}$	18.97	$\eta_{2\ O(24)}\rightarrow\sigma^*_{C(31)-H(33)}$	5.06
$\eta_{2\ O(14)}\rightarrow\sigma^*_{C(13)-O(15)}$	35.12	$\eta_{1\ O(25)}\rightarrow\sigma^*_{C(17)-C(23)}$	2.21
$\eta_{1\ O(15)}\rightarrow\sigma^*_{C(13)-O(14)}$	8.67	$\eta_{2\ O(25)}\rightarrow\sigma^*_{C(17)-C(23)}$	18.54
$\eta_{2\ O(15)}\rightarrow\pi^*_{C(13)-O(14)}$	46.39	$\eta_{2\ O(25)}\rightarrow\sigma^*_{C(23)-O(24)}$	34.57
$\eta_{2\ O(15)}\rightarrow\sigma^*_{C(13)-O(14)}$	3.50	$\eta_{2\ S(43)}\rightarrow\sigma^*_{C(34)-C(35)}$	2.97
$\eta_{2\ O(15)}\rightarrow\sigma^*_{C(33)-C(36)}$	3.56	$\eta_{2\ S(43)}\rightarrow\sigma^*_{C(34)-C(35)}$	2.96
$\eta_{2\ S(45)}\rightarrow\sigma^*_{C(33)-C(36)}$	3.05	$\eta_{2\ O(45)}\rightarrow\sigma^*_{S(43)-N(44)}$	40.60
$\eta_{2\ S(45)}\rightarrow\pi^*_{N(46)-O(47)}$	24.00		
$\eta_{2\ O(47)}\rightarrow\pi^*_{C(45)-N(46)}$	41.95		
Σ	**242.44**	**Σ**	**216.89**

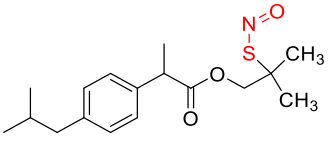

R2

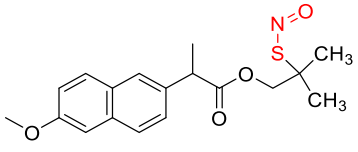

R3

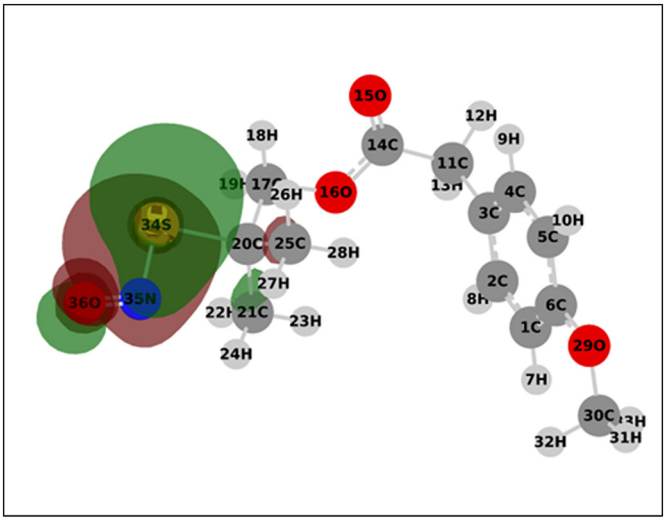

Fig. 10. $n_{O(N-O)} \rightarrow \sigma^*_{(S-N)}$ orbital interactions, with a 43.40 kcal·mol^{-1} contribution, responsible for the elongation of the S–N bond in the **R1** (X = OMe) compound.

Appendix A. Supplementary Data

The following are the supplementary data related to this article: Analysis of the stretching bands of all the investigated compounds, experimental procedures, chromatograms, spectral and characterization data. Supplementary data to this article can be found online at https://doi.org/10.1016/j.saa.2018.09.020.

References

[1] N.D. Yeomans, et al., N. Engl. J. Med. 338 (1998) 719–726.
[2] C.J. Hawkey, et al., N. Engl. J. Med. 338 (1998) 727–734.
[3] C. Bombardier, et al., N. Engl. J. Med. 23 (2000) 1520–1528.
[4] S.N. Elliott, W. Mcknight, G. Cirino, J.L. Wallace, Gastroenterology 109 (1995) 524–530.
[5] S. Fiorucci, E. Antonelli, J.L. Burgaud, A. Morelli, Drug Saf. 24 (2001) 801–811.
[6] J.L. Wallace, L.J. Ignarro, S. Fiorucci, Nat. Rev. Drug Discov. 1 (2002) 375–382.
[7] J.E. Keeble, P.K. Moore, Br. J. Pharmacol. 137 (2002) 295–310.
[8] S. Fiorucci, P. Del Soldato, Dig. Liver Dis. 35 (2003) S9–19.
[9] S. Somasundaram, S. Rafi, M. Jacob, G. Sigthorsson, T. Mahmud, R. Sherwood, A.B. Price, A. Macpherson, D. Scott, J.M. Wrigglesworth, I. Bjarnason, Gut 40 (1997) 608–613.
[10] J.L. Wallace, B. Reuter, C. Cicala, W. McKnight, M.B. Grisham, G. Cirino, Gastroenterology 107 (1994) 173–179.
[11] S. Fiorucci, L. Santucci, P. Gresele, R.M. Faccino, P. Del Soldato, A. Morelli, Gastroenterology 124 (2003) 600–607.
[12] M. Carini, G. Aldini, M. Orioli, A. Piccoli, P. Tocchetti, R.M. Facino, J. Pharm. Biomed. Anal. 35 (2004) 277–287.
[13] M. Chattopadhyay, S. Goswami, D.B. Rodes, R. Kodela, C.A. Velazquez, D. Boring, J.A. Crowell, K. Kashfi, Cancer Lett. 298 (2010) 204–2011.
[14] H.P. Monteiro, P.E. da Costa, A.K.C.A. Reis, A. Stern, Biom. J. 38 (2015) 380–388.
[15] R.J. Singh, N. Hogg, J. Joseph, B. Kalyanaraman, FEBS Lett. 360 (1995) 47–51.
[16] R.J. Singh, N. Hogg, J. Joseph, B. Kalyanaraman, J. Biol. Chem. 271 (1996) 18596–18603.
[17] S.W. Tam, et al., J. Med. Chem. 43 (2000) 4005–4016.
[18] M.A. Fernández-González, M. Marazzi, A. López-Delgado, F. Zapata, F. García-Iriepa, D. Rivero, O. Castaño, M. Temprado, L.M. Frutos, J. Chem. Theory Comput. 8 (2014) 312–323.
[19] M.D. Bartberger, K.N. Houk, S.C. Powell, J.D. Mannion, K.Y. Lo, J.S. Stamler, E.J. Toone, J. Am. Chem. Soc. 122 (2000) 5889–5890.
[20] P.R. Olivato, B. Wladislaw, S.A. Guerrero, D. Russowsky, Phosphorus Sulfur Rel. Elem. 24 (1985) 225–233.
[21] P.R. Olivato, F. Oike, J.C.D. Lopes, Phosphorus Sulfur Silicon Relat. Elem. 3-4 (1990) 391–399.
[22] D.N.S. Rodrigues, L.C. Ducati, P.R. Olivato, M. Dal Colle, J. Phys. Chem. A 119 (2015) 3823–3832.
[23] M.M. Reginato, Synthesis and Studies on the Conformational Stability of SNO-NSAIDs, Universidade Federal de São Paulo – UNIFESP, 2012 (Dissertação de Mestrado).
[24] Galactic Industries Corporation, Salem, NH, USA, 1991–1998.
[25] M.J. Frisch, G.W. Trucks, H.B. Schlegel, G.E. Scuseria, M.A. Robb, J.R. Cheeseman, G. Scalmani, V. Barone, B. Mennucci, G.A. Petersson, H. Nakatsuji, M. Caricato, X. Li, H.P. Hratchian, A.F. Izmaylov, J. Bloino, G. Zheng, J.L. Sonnenberg, M. Hada, M. Ehara, K. Toyota, R. Fukuda, J. Hasegawa, M. Ishida, T. Nakajima, Y. Honda, O. Kitao, H. Nakai, T. Vreven, J.A. Montgomery Jr., J.E. Peralta, F. Ogliaro, M.J. Bearpark, J. Heyd, E.N. Brothers, K.N. Kudin, V.N. Staroverov, R. Kobayashi, J. Normand, K. Raghavachari, A.P. Rendell, J.C. Burant, S.S. Iyengar, J. Tomasi, M. Cossi, N. Rega, N.J. Millam, M. Klene, J.E. Knox, J.B. Cross, V. Bakken, C. Adamo, J. Jaramillo, R. Gomperts, R.E. Stratmann, O. Yazyev, A.J. Austin, R. Cammi, C. Pomelli, J.W. Ochterski, R.L. Martin, K. Morokuma, V.G. Zakrzewski, G.A. Voth, P. Salvador, J.J. Dannenberg, S. Dapprich, A.D. Daniels, Ö. Farkas, J.B. Foresman, J.V. Ortiz, J. Cioslowski, D.J. Fox, Gaussian 09, Gaussian, Inc., Wallingford, CT, USA, 2009.
[26] T.K. R. Dennington, J. Millam, GaussView, Version 5, Semichem Inc., Shawnee Mission, K., 2009
[27] D.A. Zhurko, G.A. Zhurko, Chemcraft, 2014.
[28] C. Lee, C. Hill, N. Carolina, Phys. Rev. 37 (1988) 785–789.
[29] A.D. Becke, J. Chem. Phys. 98 (1993) 5648–5652.
[30] S.H. Vosko, L. Wilk, M. Nusair, Can. J. Phys. 58 (1980) 1200–1211.
[31] A.E. Reed, F. Weinhold, J. Chem. Phys. 83 (1985) 1736–1740.
[32] N.B. Colthup, L.H. Daly, S.E. Wiberly, Introduction to Infrared and Raman Spectroscopy, 3rd ed. Academic Press, San Diego, 1990.
[33] M.J.S. Dewar, E.G. Zoebisch, E.F. Healy, J.J.P. Stewart, J. Am. Chem. Soc. 107 (1985) 3902–3909.
[34] B. Wang, G.P. Ford, J. Comp. Chem. 15 (1994) 200–207.
[35] C. Baciu, J.W. Gauld, J. Phys. Chem. A 107 (2003) 9946–9952.
[36] M. Marazzi, A. Lopez-Delgado, M.A. Fernandez-Gonzalez, O. Castano, L.M. Frutos, M. Temprado, J. Chem. Theory Comput. 8 (2012) 3293–3302.
[37] B. Meyer, A. Genoni, A. Boudier, P. Leroy, M.F. Ruiz-Lopez, J. Phys. Chem. A 120 (2016) 4191–4200.
[38] A. Cánneva, C.A.O. Della Védova, N.W. Mitzel, M.F. Erben, J. Phys. Chem. A 119 (2015) 1524–1533.
[39] J. Yi, M.A. Khan, J. Lee, G.B. Richter-Addo, Nitric Oxide 12 (2005) 261–266.
[40] Dmitry G. Khomyakov, Qadir K. Timerghazin, J. Chem. Phys. 147 (2017), 044305. (1–13).
[41] A. Cánneva, M.F. Erben, R.M. Romano, Y.V. Vishnevskiy, C.G. Reuter, N.W. Mitzel, C.O. Della Védova, Chem. Eur. J. 21 (2015) 10436–10442.
[42] A. Cánneva, R.L. Cavasso-Filho, R.M. Romano, C.O. Della Védova, S. Tong, M. Ge, M.F. Erben, Chemistry Select 2 (2017) 2021–2027.
[43] T.A. Heinrich, R.S. da Silva, K.M. Miranda, C.H. Switzer, D.A. Wink, J.A. Fukuto, Br. J. Pharmacol. 169 (2013) 1417–1429.
[44] D.R. Arnelle, J.S. Stamler, Arch. Biochem. Biophys. 318 (1995) 279–285.